

Dynamics of the Excited States of *p*-Terphenyl and Tetracene: Solute–Solvent Interaction

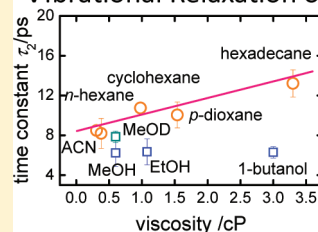
Kuan-Lin Liu, Yi-Ting Chen, Hsing-Hui Lin, Che-Sheng Hsu, Hao-Wei Chang, and I-Chia Chen*

Department of Chemistry, National Tsing Hua University, Hsinchu, Taiwan 30013, Republic of China

Supporting Information

ABSTRACT: The time-resolved fluorescence of *p*-terphenyl, 2,2''-dimethyl-*p*-terphenyl (*dm*-terphenyl), and tetracene dissolved in solvents was measured with fluorescence up-conversion and time-correlated single-photon counting. We characterized the relaxation dynamics of vibrational energy in these three molecules by examining their properties in solvents of varied physical properties. According to the measured curves of fluorescence decays obtained at excitation wavelength 266/256 nm, we propose that *p*-terphenyl and *dm*-terphenyl both undergo initially an ultrafast intramolecular redistribution of vibrational energy. A conformational relaxation of *p*-terphenyl in excited-state S_1 with time constant 6–13 ps is proposed from its linear dependence on the viscosity of solvents. This process and vibrational energy relaxation are accelerated in a protic solvent involving efficient coupling to the high-energy bath modes of the solvent. Because the torsional conformational change of *dm*-terphenyl is effectively inhibited by the steric hindrance imposed by its methyl substituents, its vibrational relaxation is found to be independent of the viscosity of the solvent but remains rapid with time constant 5.2–8.8 ps. The time constant of vibrational relaxation in tetracene is observed to be 12–16 ps, with no evident dependence on solvent viscosity or thermal diffusivity. The fact that accepting modes with greater energy are more effective in transferring energy for a system with a large excess of vibrational energy is proposed to explain the ratio of the rates of vibrational relaxation for methanol MeOH/MeOD ≈ 2 .

Vibrational Relaxation of *p*-Terphenyl



1. INTRODUCTION

Following photoexcitation of a molecule in the condensed phase, excess excitation energy is redistributed internally and transferred to the solvent environment on a time scale of picosecond or less, which is typically accompanied by an altered molecular geometry and solvent reorganization.^{1–3} The effects of a solvent on the molecular dynamics in the excited state, and, in particular, the microscopic mechanisms dictating their time scales, remain the central topic in a condensed phase.^{4–7} Time-resolved fluorescence and transient-absorption experiments are techniques commonly performed in monitoring the rates of deactivation of an excited molecule in various solvents. These rates are then compared with the solvent bulk properties to elucidate the dominant process of relaxation.

It is widely accepted that for flexible aromatic molecules in solution the oligophenyls have nonplanar geometries in their ground state but that they undergo a conformational alteration on photoexcitation to their low-lying electronic states, typically from aromatic toward quinoidal geometries.^{8,9} An improved understanding of the conformational relaxation of these oligophenyls is essential for their use in optoelectronic applications.^{10,11} Biphenyl in its ground state has a dihedral angle determined to be $\sim 42^\circ$ in the minimum torsional potential energy, whereas its first excited state is planar.¹² Mank et al. measured transient absorption spectra of biphenyl and identified two time constants, 400 fs and 12 ps, in the decay curves, assigned to correlated conformational relaxation;¹³ this biphasic conformational relaxation implies that

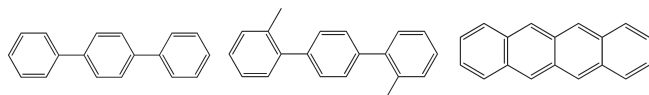
multiple nuclear coordinates are involved. Leonard and Gustafson used time-resolved Raman spectra to investigate the relaxation dynamics of trans-4,4'-diphenylstilbene (DPS);¹⁴ an excited state S_1 evolved with vibrational and conformational relaxation, the latter of which involved a conversion from a nonplanar ground state to a planar excited state in the biphenyl moiety. According to an analysis of transient absorption spectra of DPS, Tan and Gustafson correlated the rates of vibrational relaxation with the thermal diffusivity of the solvent, whereas the conformational relaxation was affected by both the viscosity and dielectric constant of the solvent.¹⁵ The dependence on thermal diffusivity arose from the dissipation of heat from the hot solute to the surrounding solvent molecules; the subsequent transport of energy within the solvent was treated as a classical heat conduction process.

Excitation of [(1,1-biphenyl)-4,4'-diyl-di-2,1-ethenediyl]bis-(dimethylsilane) at 266 nm caused the molecule to undergo conformational relaxation in state S_1 , which was accelerated in protic solvents;¹⁶ the rate of conformational relaxation, which was accompanied by vibrational cooling, varied with the viscosity of the solvent. In protic solvents, forming H-bonding with the solute tended to favor vibrational relaxation,^{17,18} but H-bonding of this biphenyl does not occur; this rate was proposed to increase because of enhanced conformational + vibrational relaxation

Received: April 24, 2011

Revised: September 4, 2011

Published: October 26, 2011

Scheme 1. Molecular Structures of *p*-Terphenyl, *dm*-Terphenyl, and Tetracene

through an interaction with the high-energy O–H librational motions of solvent molecules. All this work revealed that the solvent environment plays multiple roles in governing the dynamics of relaxation in excited states.

To investigate further the effect of the nature of the solvent, we measured the femtosecond time-resolved fluorescence of *p*-terphenyl, 2,2''-dimethyl-*p*-terphenyl (*dm*-terphenyl), and tetracene (structures shown in Scheme 1) in solvents with varied physical properties—viscosity, dielectric constant, and protic nature. Experiments and calculations indicate that in both gaseous and solution phases *p*-terphenyl is twisted in the ground state but planar in excited-state S_1 .^{17,18,21,22} The equilibrium geometric change on photoexcitation and the simple and symmetrical structure make *p*-terphenyl a suitable candidate for study of solute–solvent interactions, especially with protic solvents. The twisting motion of *dm*-terphenyl to become planarity like biphenyl is hindered by the methyl substituents, which thus provides a test of the effect of solute–solvent interaction for this motion. Tetracene has a rigid molecular structure, thus lacking the torsional degree of freedom of biphenyls. Sarkar et al.²³ measured femtosecond fluorescence anisotropy and intensity to probe the electronic and vibrational relaxation of tetracene in nonpolar solvents. We investigated its vibrational relaxation in protic solvents as a further test of the structural dependence of solute–solvent interaction.

2. EXPERIMENTAL SECTION

2.1. Samples. *p*-Terphenyl (99.5+%), tetracene (98%) (both from Aldrich), and *dm*-terphenyl (Lambda Physik, dye LC3300) were used as received. For time-resolved measurements, typical concentrations were 10^{-5} to 10^{-4} M. Spectroscopic grade *n*-hexane, cyclohexane, hexadecane, *p*-dioxane, acetonitrile, methanol (MeOH), deuterated methanol (CH_3OD , MeOD), perdeuterated methanol (CD_3OD), ethanol, and 1-butanol (Aldrich) were used as received. The steady-state absorption (Hitachi U3300 spectrometer) and fluorescence (Hitachi F4500 fluorimeter) spectra were recorded with the indicated instruments. For time-resolved measurements, the power of the laser for excitation was maintained below 2 mW; absorption spectra were recorded before and after measurements to ensure that no sample degradation had occurred. The absorbance of the solution for fluorescence up-conversion measurements was normally small and kept below ≤ 0.5 at the excitation wavelength for low emission efficiency sample like tetracene. For time-correlated single-photon counting (TCSPC) measurements, we avoided aggregation to attain the S_1 lifetime with low concentrations and matched the same conditions as those in the up-conversion experiments for fitting the time components with large concentrations.

2.2. Fluorescence Up-Conversion System. The laser system and setup for fluorescence up-conversion measurements are described as follows. The light source is a femtosecond mode-locked Ti:sapphire laser (Spectra-Physics, Mai Tai) pumped with a Nd:YVO₄ laser (5 W cw, 532 nm, Spectra-Physics, Millennia-type);

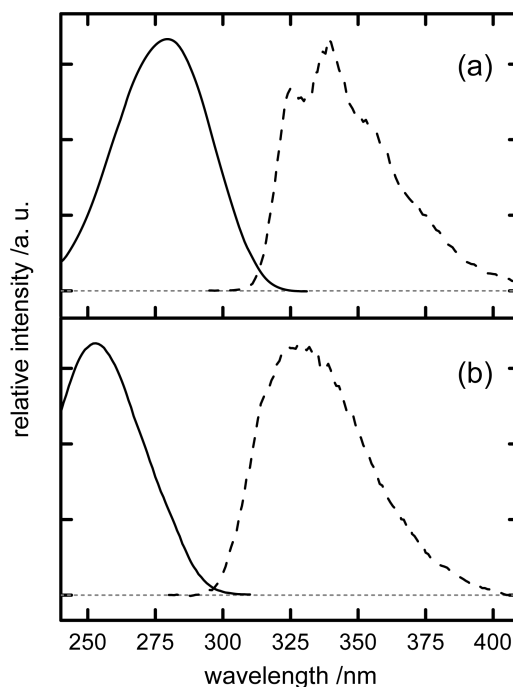


Figure 1. Absorption (solid) and fluorescence spectra (dashed) of (a) *p*-terphenyl and (b) *dm*-terphenyl in acetonitrile.

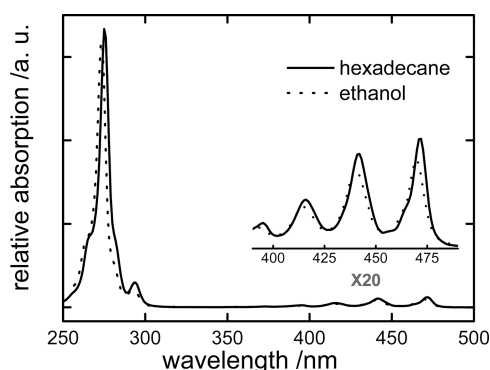
this laser outputs a pulse train (82 MHz, 800 nm) with average power ~ 400 mW. The third-harmonic pulses at wavelength either 256 or 266 nm were generated with two nonlinear crystals (BBO, type I) and were focused with a lens (focal length 50 mm) onto a rotating sample cell (path length 1 mm) for excitation. The residual fundamental pulse served as an optical gate. Detections of the fluorescence at the magic-angle, parallel, and perpendicular conditions were achieved on rotating the excitation polarization with respect to the polarization of gate pulses. The fluorescence was collected and focused onto a sum-frequency generation crystal (BBO, type I) with off-axis parabolic mirrors (focal lengths 5 and 7 cm at 90°). After traversing a variable delay stage, the gate pulse was noncollinearly ($\sim 12^\circ$) focused with a lens (focal length 10 cm) onto a sum-frequency generation crystal (BBO, type I). The sum-frequency signal was collected with a lens and separated from other light by means of an iris and a band-pass filter and then entered a double monochromator. The signal was detected with a photomultiplier tube in combination with a photon counter. Various emission wavelengths were selected on rotating the SFG crystal and tuning the monochromator.

The instrument response function was obtained on measuring the ultrafast S_2 fluorescence of *trans*-azobenzene at 380 nm; this fluorescence decay appeared with a symmetric Gaussian shape of which the full width at half-maximum (fwhm) was ~ 230 fs.²⁴ For terphenyl and tetracene, the up-conversion curves displayed here were averaged over about four and ten spectra, respectively, and each spectrum consists of one forward and one backward scan; each data point in a scan was averaged over 3 s.

2.3. Time-Correlated Single-Photon Counting. Picosecond time-resolved fluorescence was measured with TCSPC. The light source was the same laser system as that for the measurement of fluorescence up-conversion. A small fraction of the generated third harmonic (266 nm) served as an excitation source. A sample

Table 1. Dielectric Constant, ϵ_r , Viscosity, η (cP), and Thermal Diffusivity, D_T ($10^7 \text{ m}^2 \text{ s}^{-1}$), of Solvent, Maximal Peak Position (nanometers) in Steady-State Absorption, A_{max} (nm), and Emission, F_{max} (nm), Spectra

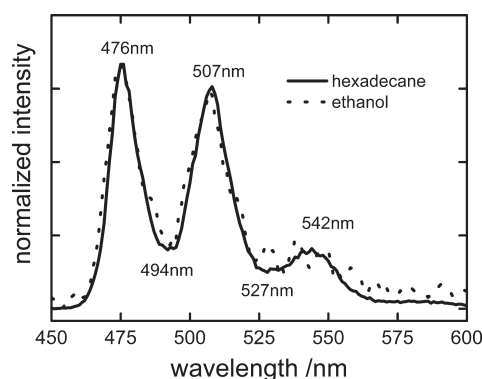
solvent	ϵ_r	η	D_T	<i>p</i> -terphenyl		<i>dm</i> -terphenyl		tetracene	
				A_{max}	F_{max}	A_{max}	F_{max}	A_{max}	F_{max}
<i>n</i> -hexane	1.90	0.31	0.807	276	324, 338	250	327		
cyclohexane	2.02	0.98	0.858	276	326, 340	251	327		
hexadecane	2.05	3.34	0.841	279	328, 341	252	327	416, 442, 472	476, 508
<i>p</i> -dioxane	2.21	1.54	0.891	281	327, 342	254	329		
acetonitrile	38.8	0.38	1.075	280	325, 339	253	329	416, 441, 471	476, 507
methanol	32.6	0.60	0.998	278	325, 339	241	329	414, 440, 469	475, 506
ethanol	24.4	1.08	0.878	278	326, 340	251	328	415, 441, 471	475, 507
1-butanol	18.2	3.00	0.79	279	326, 340	252	330	416, 442, 471	477, 509

**Figure 2.** Steady-state absorption spectra of tetracene in hexadecane (solid line) and in ethanol (dotted line).

was contained in a cuvette (path length 1 mm). The concentrations were varied from those used at up-conversion experiments to diluted conditions. The fluorescence was filtered with a bandpass filter (± 10 nm) and detected with a multichannel plate photomultiplier (MCP-PMT, Hamamatsu). A vertical polarizer was placed before the MCP-PMT, and the polarization of the pump beam was rotated to achieve the magic-angle condition. The instrument response function was ~ 30 ps at fwhm.

3. RESULTS AND KINETIC MODELING

3.1. Steady-State Electronic Absorption and Emission Spectra. The absorption and fluorescence spectra of *p*-terphenyl and *dm*-terphenyl in acetonitrile are presented in Figure 1a,b. *p*-Terphenyl shows a strong and structureless π - π^* absorption with maximum at ~ 280 nm; its fluorescence centered at ~ 339 nm exhibits a prominent vibronic progression of interval $\sim 1271 \text{ cm}^{-1}$ that is related to the C–C stretching mode in the phenyl ring. This feature is typical of a molecule exhibiting torsional disorder in the ground state but a planar excited state, which also results in the loss of the mirror image between the absorption and fluorescence profiles.^{25,26} The steric hindrance, posed by the methyl substituents of *dm*-terphenyl has a clear effect on the steady-state spectra. The absorption and emission maxima of *dm*-terphenyl, relative to those of *p*-terphenyl, are blue-shifted to ~ 250 and ~ 328 nm, respectively. The featureless absorption and fluorescence profiles become mirror-imaged, which implies a twisted geometry for both the ground and first

**Figure 3.** Steady-state fluorescence spectra of tetracene in hexadecane and in ethanol with 266-nm excitation; the detection wavelengths of fluorescence up-conversion measurements are indicated.

excited states. In all solvents, including both protic and aprotic, the steady-state spectra of *p*- and *dm*-terphenyl display features similar to those described above, indicating no particular solvent dynamics in these compounds. Their peak positions are listed in Table 1.

The absorption spectra of tetracene in hexadecane and in ethanol are displayed in Figure 2. In these spectra, a sharp and intense absorption line at 276 nm is assigned as transition $S_0 \rightarrow {}^1B_b$. A weak absorption system showing a clear vibronic progression (spacing $\sim 1400 \text{ cm}^{-1}$) in the range 400–475 nm marks transition $S_0 \rightarrow {}^1L_a$. The transition dipole moments of these $S_0 \rightarrow {}^1B_b$ and $S_0 \rightarrow {}^1L_a$ transitions are parallel to the long and short axes of the molecule, respectively.²³ A third absorption system $S_0 \rightarrow {}^1L_b$, located in a region of energy slightly greater than that of transition $S_0 \rightarrow {}^1L_a$, is unobserved because of a small oscillator strength. Time-dependent density-functional theory (TD-DFT) calculations at level B3LYP/6-311G(d) using Gaussian package²⁷ indicate that transition $S_0 \rightarrow {}^1L_b$ lies at ~ 374 nm with oscillator strength 0.038. Figure 3 shows curves for the fluorescence of tetracene in hexadecane and in ethanol. With excitation at 266 nm, the fluorescence in the range 470–530 nm exhibits a clear vibronic structure and a mirror image of the $S_0 \rightarrow {}^1L_a$ band, indicating that this fluorescence originates from the lowest excited state 1L_a . Table 1 lists the absorption and fluorescence maxima in solvent acetonitrile, methanol, ethanol, 1-butanol, and hexadecane; in these solvents, the shapes and

Table 2. Summary of Fitted Time Constant of the Time-Resolved Fluorescence for *p*-Terphenyl

solvent	τ_1/ps	τ_2/ps	τ_3/ns
<i>n</i> -hexane	0.09–0.17	8.5 ± 0.6	1.06 ± 0.01
cyclohexane	0.09–0.13	10.8 ± 0.5	1.01 ± 0.02
hexadecane	0.07–0.17	13.2 ± 0.8	1.09 ± 0.01
<i>p</i> -dioxane	0.08–0.13	10.1 ± 1.3	1.04 ± 0.01
acetonitrile	0.08–0.19	8.2 ± 1.5	1.20 ± 0.02
methanol	0.06–0.15	6.2 ± 1.3	1.22 ± 0.01
ethanol	0.11–0.16	6.3 ± 1.3	1.18 ± 0.03
1-butanol	0.13–0.16	6.3 ± 0.4	1.11 ± 0.01
methanol-OD	0.1–0.2	7.9 ± 0.7	1.18 ± 0.02

Table 3. Summary of Fitted Time Constants of the Time-Resolved Fluorescence for *dm*-Terphenyl

solvent	τ_1/ps	τ_2/ps	τ_3/ns
<i>n</i> -hexane	0.2–0.4	6.9 ± 0.3	1.02 ± 0.01
cyclohexane	0.2–0.3	6.2 ± 0.6	1.03 ± 0.01
hexadecane	0.2–0.3	7.6 ± 1.4	1.05 ± 0.01
<i>p</i> -dioxane	0.2–0.3	5.4 ± 0.8	1.06 ± 0.01
acetonitrile	0.2–0.4	5.4 ± 0.4	1.11 ± 0.01
methanol	0.2–0.3	5.2 ± 0.7	1.12 ± 0.01
ethanol	0.2–0.3	5.8 ± 0.5	1.11 ± 0.01
1-butanol	0.2–0.3	6.2 ± 0.6	1.10 ± 0.01
methanol-OD	0.3–0.4	8.8 ± 0.6	1.21 ± 0.05

positions of the steady-state spectra are similar, and spectral shifts <3 nm indicate little solvent dynamics.

3.2. TCSPC Nano-Picosecond Fluorescence Measurements.

Fluorescence lifetimes of *p*- and *dm*-terphenyl, excited at 266 and 256 nm, respectively, were collected within wavelength range 310–380 nm. In all solvents, exponential decay curves were derived for both molecules; the fitted time constants from the TCSPC curves are listed in Tables 2 and 3 as τ_3 . Selected fluorescence decay curves of *p*-terphenyl are displayed in Figure 4. The fluorescence lifetimes of *p*- and *dm*-terphenyl both increase with the dielectric constant of solvent, as illustrated in the inset of Figure 4. The slightly shorter lifetimes of both molecules in nonpolar solvents implies a relatively nonpolar nature of their excited states. Fluorescence decays of tetracene were measured at wavelengths 480, 500, and 540 nm; all emission curves decay similarly in this temporal range at the detected wavelengths. The fitted time constants measured at varied solvents are listed in Table 4 as τ_3 . The obtained fluorescence lifetime is slightly lengthened in nonpolar solvent, hexadecane ~5.2 ns, but nearly invariant in polar solvents (4.4 ns). For these three compounds, time constant τ_3 obtained in protic (MeOH) and aprotic (acetonitrile) solvents with similar dielectric constant is not varied, which indicates that H bonding exerts no effect in τ_3 .

3.3. Femtosecond Fluorescence Measurements. The fluorescence up-conversion curves of *p*-terphenyl were recorded with excitation at 266 nm and detection at 330, 340, and 360 nm, which correspond to the fluorescence of S_1 . Figure 5 shows the femtosecond time-resolved fluorescence of *p*-terphenyl in acetonitrile; a rapid rise followed by a slow rise is observed in each case at each detection wavelength. The measured curves for the other solvents are displayed in the Supporting Information. Calculations of vertical excitation energies, with TD-DFT at

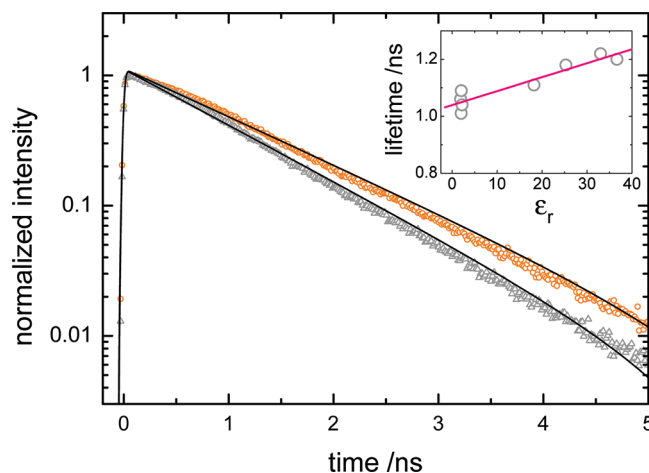


Figure 4. Selected fluorescence decay curves of *p*-terphenyl in acetonitrile (circle) and cyclohexane (triangle) with 266 nm excitation and 380 nm detection. The inset illustrates a correlation between fluorescence lifetime and dielectric constant of the solvent.

Table 4. Summary of Fitted Time Constants of the Time-Resolved Fluorescence for Tetracene

solvent	τ_1/ps	τ_2/ps	τ_3/ns
hexadecane	0.11 ± 0.03	16.4 ± 2.1	5.2 ± 0.2
acetonitrile	0.11 ± 0.02	11.8 ± 1.4	4.2 ± 0.1
methanol	0.08 ± 0.07	15.8 ± 4.8	4.4 ± 0.1
ethanol	0.07 ± 0.01	16.6 ± 4.0	4.5 ± 0.1
methanol-OD	0.13 ± 0.03	33.1 ± 3.4	4.2 ± 0.1
methanol- d_4	0.14 ± 0.02	33.1 ± 4.6	4.2 ± 0.1
1-butanol	0.07 ± 0.01	13.5 ± 1.4	4.4 ± 0.1

level B3LYP/6-311G(d), indicate that *p*-terphenyl populates the S_1 upon excitation at 266 nm, which is also justified by the measurement of anisotropy. The anisotropy r is defined as

$$r(t) = (I_{\parallel} - I_{\perp}) / (I_{\parallel} + 2I_{\perp}) \quad (1)$$

involving intensities with polarizations parallel (I_{\parallel}) and perpendicular (I_{\perp}) between the pump beam and the fluorescence. At time zero, $r_0 \approx 0.35$ with a decay near 80 ps indicates that the accessed electronic state is the emitting state and the decay is mainly originated from rotational diffusion. The deviation of the experimental value from theoretical one (0.4) is due to the finite solid angle of fluorescence collection that induces some contribution from the other polarization component.

We applied this kinetic model to fit the experimental data



in which $S_{1,FC}$, S_1^* , and S_1 represent the initially populated Franck–Condon region, the vibrationally hot, and the relaxed first excited state, respectively; S_0 denotes the ground state. According to the fitting method, the necessary variables to fit globally the experimental curves result from iterative deconvolution of the instrument response function with multiple exponential function. Fluorescence lifetime τ_3 was fixed to the value obtained from TCSPC measurements. The direct evaluation of the rise component τ_1 was performed on individual curves at varied detection wavelengths. The value of τ_2 was obtained from

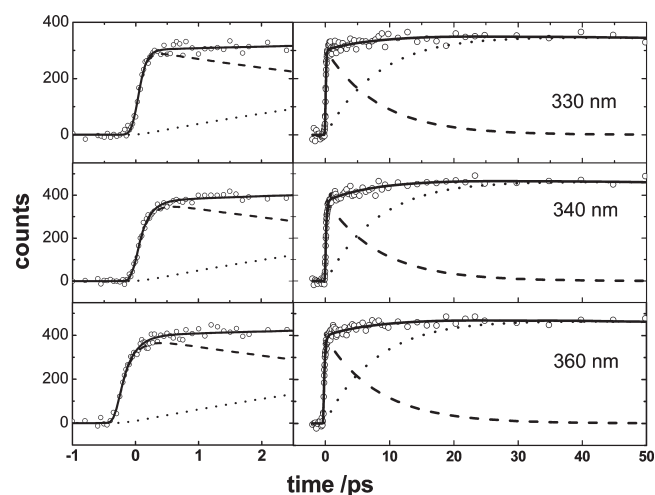


Figure 5. Femtosecond time-resolved fluorescence decay curves of *p*-terphenyl in acetonitrile, detected at the indicated wavelength. Open circles and dashed, dotted, and solid lines are experimental data, the best fitted curve for S_1^* and S_1 components, and the overall fitted curve, respectively.

the best fit to the experimental curves for all detection wavelengths. We assume that many vibrational modes are involved, yielding an averaged relaxation rate. The results of fits are summarized in Table 2. The initial ultrafast rise τ_1 (0.06 to 0.13 ps) increases slightly with emission wavelength. The slower rise τ_2 is 8.2–13.2 ps in an aprotic solvent and is short 6.2 to 6.3 ps in a protic solvent, but becomes greater 7.9 ps in deuterated methanol-OD. The results of fits are summarized in Table 2.

The time-resolved fluorescence of *dm*-terphenyl is obtained on fluorescence up-conversion with excitation at 256 nm. The altered excitation wavelength was intended to store vibrational energy ($\sim 5300\text{ cm}^{-1}$) similar to that in *p*-terphenyl (5600 cm^{-1}). The detection wavelengths are within 310–370 nm, for which emission arises from S_1 state. Figure 6 displays the femtosecond time-resolved fluorescence curves of *dm*-terphenyl in acetonitrile and the curves in methanol-OD are similar and are shown in the Supporting Information. The temporal behaviors of fluorescence decay of *dm*-terphenyl are similar to those of *p*-terphenyl, that is, a biphasic rise, followed by a long decay. The results of calculations of vertical excitation energies with TD-DFT (B3LYP/6-311G(d)) show that S_1 excited state is populated on excitation at 256 nm. The experimental curves were accordingly fitted with the same kinetic model described in eq 2, with the fitting method the same as that for *p*-terphenyl. The initial rapid rise τ_1 0.2 to 0.4 ps increases with emission wavelength and is slightly greater than those for *p*-terphenyl. In protic and aprotic solvents, the slower rise τ_2 is obtained to be 5.2–8.8 ps. However, τ_2 obtained in methanol-OD is ~ 1.7 times greater than that in methanol. The results for those time constants obtained for various solvents are listed in Table 3.

The fluorescence up-conversion curves of tetracene were recorded with excitation at 266 nm and detection at 476, 494, 507, 527, and 542 nm, which correspond to crests and troughs in the S_1 (1L_a) fluorescence curves. (See Figure 3.) Figure 7 shows the femtosecond time-resolved fluorescence of tetracene in ethanol. An ultrarapid rise is observed in each case at each detection wavelength. Because tetracene was initially prepared in the S_3 (1B_b) excited state, this rise is assigned to an electronic conversion

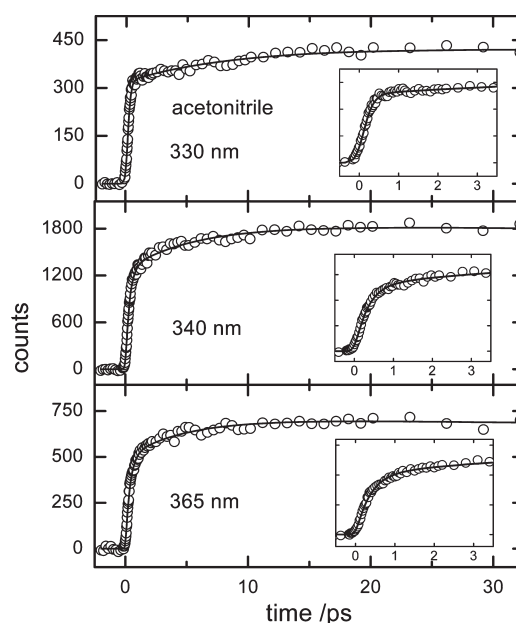


Figure 6. Femtosecond time-resolved fluorescence decay curves of *dm*-terphenyl in acetonitrile at 330, 340, and 365 nm. The open circles and the black solid curves are experimental data and the best fitted curves, respectively. The insets show the early time fluorescence rise.

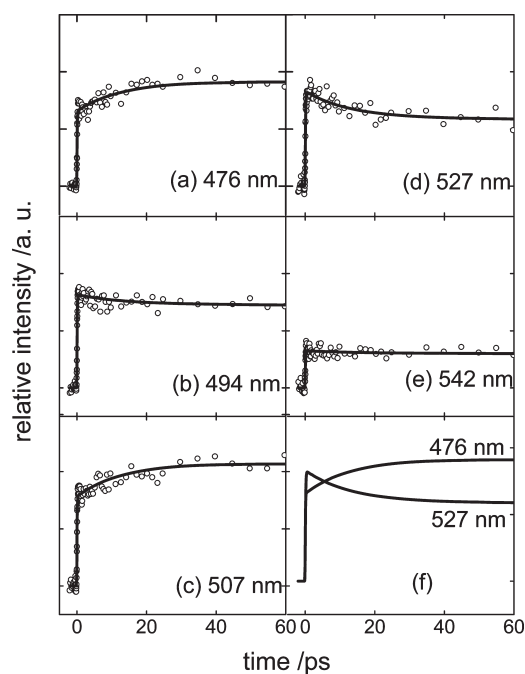


Figure 7. Femtosecond time-resolved fluorescence decay curves of tetracene in ethanol at (a) 476, (b) 494, (c) 507, (d) 527, and (e) 542 nm. The open circles and solid curves are experimental data and the best fitted curves, respectively. (f) Fitted curves at detection wavelength 476 and 527 nm are shown for demonstration of spectral evolution.

$S_3 \rightarrow S_1$ (1L_a). Sarkar et al.²³ measured the fluorescence anisotropy from the S_3 and the S_1 states; from the agreement of decay and rise of fluorescence intensity, they proposed that state 1B_b is vibronically coupled to state 1L_a with a conversion lifetime ~ 100 fs. Our measurements show a similar electronic conversion

with rates near those in nonpolar solvents. In the picosecond region, a several-picosecond component appeared with rise at 476 and 507 nm (corresponding to crests) and decay at 494, 527, and 542 nm (troughs) for most solvents used in the present work, except acetonitrile for which only decay curves were detected (shown in the Supporting Information). Because the detection wavelengths are within the S_1 fluorescence, the rise and decay features originated not from population dynamics but from spectral changes of the S_1 fluorescence. The troughs in the emission curves correspond to the positions of hot bands and the crests correspond to bands from lower energies accounting for the observations of the rise and decay behavior in the femtosecond measurements. In acetonitrile, the rapid relaxation shows only decays dominantly in the fluorescence curves.

The following kinetic model fits the experimental curves for all wavelengths



in which S_3 is the initially populated excited state. The large fluorescence lifetime τ_3 again is fixed to the value obtained from TCSPC measurements. Because similar decay time constants τ_2 are displayed in the experimental curves at varied detection wavelengths, only one averaged value of τ_2 from the best fits of the rise and decay curves is obtained. The ultrafast rise τ_1 is 70–140 fs, and the slow component τ_2 ranges between 8.6 and 15.7 ps. We observed a large isotopic effect in solvent MeOD and perdeuterated methanol, for which $\tau_2 \approx 33.1$ ps, respectively. The fitted time constants are summarized in Table 4.

4. DISCUSSION

4.1. Excited-State Dynamics of *p*- and *dm*-Terphenyl. The initial ultrafast rise τ_1 for *p*- and *dm*-terphenyl is assigned to an intramolecular vibrational redistribution (IVR). This slightly wavelength-dependent IVR process has been reported for various chromophores with similar chemical structures.^{28,29} Possibly the states near Franck–Condon region of S_1 for *p*- and *dm*-terphenyl are initially coupled to some varied vibrational levels of the accepting modes, which in turn result in multiple relaxation rates ($1/\tau_1$) and emit light at varied wavelengths. Nonetheless, processes resulting from dynamic response between the solvent environment and chromophore, for example, inertial component of solvation,^{30–33} cannot be excluded under the current experimental resolution. In view of the nearly invariant steady-state spectra of both *p*- and *dm*-terphenyl in solvents varied largely in dielectric constant as well as polarity, the contribution of the solvation process should be minimal. Ultrafast solvation process for *p*-terphenyl in ethanol and cyclohexane is observed with photon echo experiment but is absent in both solvents using the fluorescence up-conversion technique because of very weak solute–solvent interaction and specific sensitivity of photon echo signal to the solvent dynamics.³⁴ It has been shown that the methyl or phenyl substituents on aromatic molecules could enhance the rate of IVR.^{35,36} However, adding these methyl groups somewhat decreases the rate of IVR in *dm*-terphenyl.

The slower rise τ_2 observed in the fluorescence of *p*-terphenyl in aprotic solvents correlates linearly with solvent viscosity, as shown in Figure 8, which indicates that it moves from the Franck–Condon region (twisted structure) toward a planar geometry in the S_1 state, as expected for biphenyl-like molecule. In protic solvents, however, τ_2 (~ 6.2 ps) decreases and shows a

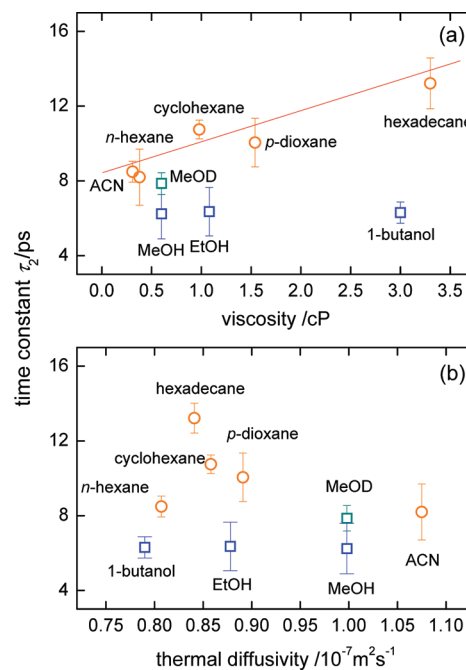


Figure 8. Relaxation time constant τ_2 in aprotic (circle) and protic (square) solvents versus viscosity and thermal diffusivity of solvent for *p*-terphenyl. A linear correlation between τ_2 and viscosity for aprotic solvents is exhibited.

clear dependence on neither solvent viscosity nor dielectric constant. Because acetonitrile has an even greater dielectric constant but a smaller viscosity than 1-butanol, we exclude a possibility of effects on τ_2 induced by the polarity variation. The shapes and positions of steady-state spectra are similar in both protic and aprotic solvents. We reasonably assume that *p*-terphenyl in protic solvents also adopts a planar geometry in excited-state S_1 but the conformational relaxation is accelerated.

Iwata and Hamaguchi reported a systematic study on the vibrational cooling of S_1 *trans*-stilbene in solution with time-resolved Raman spectroscopy, and they found a clear correlation between the cooling rate of the solute and the thermal diffusivity of the solvent.³⁷ For the three molecules under investigation here, however, none of them is shown to correlate with the thermal diffusivity of the solvent, as illustrated in Figures 8–10, which implies that this macroscopic property of solvent is inadequate to dictate their deactivation processes.^{16,38}

It is widely accepted that the excess vibrational energy either is transferable to the solvent bath modes or participates in a resonant transfer to solvent vibrations with similar vibrational frequencies.^{39,40} Also called friction spectra, the spectral distribution of the bath modes of solvent is continuous and highly dense, which plays a major role in the vibrational cooling in most cases.^{41–43} For polyatomic molecules, an increased rate of vibrational relaxation in protic solvents has been reported by several groups. Vibrational relaxation of betaine 30 in the ground state is increased in a protic solvent, with a linear correlation between the rates and several vibrational modes through IVR; the rate of IVR varies with the molar number of OH groups per unit volume of solvent.⁴⁴ The formation and dissociation of H-bonding between betaine 30 and solvent provide extra degrees of freedom for dissipation of energy. For azulene, the rate of vibrational relaxation also increased in protic solvents. Most examples of

such a dependence of rate of vibrational relaxation on solvent are for the ground state, but for azulene, this enhancement was found for both S_2 and S_0 states.^{45–47} Middleton et al. further reported the rate of vibrational relaxation of 9-methyladenine to be enhanced in solvents with H bonds: the rate for H_2O is ~ 1.8 times that for D_2O . Given the friction spectra of H_2O and D_2O , they concluded that this increase arose because the proportion of solvent modes at wavenumber $>700\text{ cm}^{-1}$ in H_2O has a greater intensity, which facilitates the energy relaxation of vibrational modes between 1400 and 1800 cm^{-1} .⁴⁸

The observation of decreased τ_2 for *p*-terphenyl in protic solvent can be explained by the enhanced rate of vibrational relaxation. One or more vibrational modes that couple to conformational relaxation are also likely to mediate the excess energy to the solvent. We also examined the solvent isotope effect by measuring the time-resolved fluorescence of *p*-terphenyl in methanol-OD; time constant τ_2 obtained in methanol-OD is ~ 1.3 times that in methanol. In solvent methanol, the low-frequency vibrational modes arise mainly from hindered translations, which vary insignificantly because of small isotopic effects on molecular mass, but the librational motion, which is responsible for the high-frequency region in the friction spectra and is absent in aprotic solvents, alters from ~ 655 (MeOH) to 475 cm^{-1} (MeOD).^{49–52} Because both the librational frequency and their ratios for MeOH/MeOD are near those of H_2O/D_2O , the influence of the isotope change on the large-wavenumber region of the friction spectra is thus expected to be qualitatively similar. This indicates that the vibrational modes with frequency within ca. $700\text{--}1000\text{ cm}^{-1}$ are candidates for dissipating excess energy for *p*-terphenyl in the first excited state. This conclusion is further supported by the picosecond time-resolved Raman experiment on S_1 *p*-terphenyl; an in-plane ring vibration at 750 cm^{-1} exhibits a peak position shift and a narrowing bandwidth simultaneously within 40 ps , which is indicative of a vibrational relaxation process and a concomitant conformational change.⁵³

The methyl substituents of *dm*-terphenyl have a large impact on the slower dynamics in its S_1 state. In protic and aprotic solvents, the time constant τ_2 ($5.2\text{--}8.8\text{ ps}$) is insensitive to solvent viscosity (Figure 9), indicating that conformational relaxation of twisted motion is effectively inhibited by the methyl groups. From the unaltered steady-state spectra in solvents varied largely in dielectric constant as well as polarity, the solvent dynamics is unlikely to account for this several picoseconds dynamics. Because of similar molecular structure to *p*-terphenyl, the time constant τ_2 is assigned to the vibrational relaxation process. It is noted that the value τ_2 is smaller than that observed in *p*-terphenyl in the same solvent, showing that the energy dissipation is more effectively and become less responsive to the O–H motion in protic solvent. Nevertheless, a similar isotopic effect is observed for *dm*-terphenyl; the time constant τ_2 obtained in methanol-OD is ~ 1.7 times greater than that in methanol, which again can be attributed to varied friction spectra of MeOH and MeOD within ca. $700\text{--}1000\text{ cm}^{-1}$. This shows that the torsional motions of the methyl substituents, in addition to some vibrational modes with frequency within $700\text{--}1000\text{ cm}^{-1}$, possibly participate in the vibrational relaxation process.

4.2. Excited-State Dynamics of Tetracene. Sarkar et al. reported detailed studies of the photophysics of S_1 tetracene in nonpolar solvent:²³ (i) a rapid rise appeared globally in S_1 fluorescence is assigned to the $^1B_b \rightarrow ^1L_a$ internal conversion, followed by IVR process, and (ii) a slower time constant shows either decay or rise behaviors, originated from the spectral change,

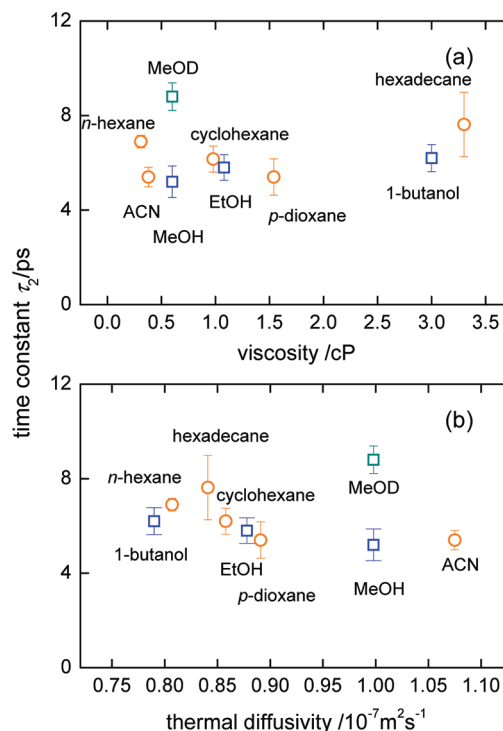


Figure 9. Relaxation time constant τ_2 of *dm*-terphenyl in aprotic (circle) and protic (square) solvents versus (a) viscosity and (b) thermal diffusivity.

are assigned to the vibrational relaxation process. We further explore the photophysics of tetracene in polar solvents. The initial ultrafast rise τ_1 is relatively unaltered with solvent change, which implies that the energy gap between 1B_b and 1L_a is insensitive to solvent environments according to the energy gap law.⁵⁴ The slow component τ_2 ranges between 8.6 and 15.7 ps and shows no clear correlation with thermal diffusivity but a slight dependence on the viscosity, as illustrated in Figure 10. The value of τ_2 is similar to the reported ones²³ and is thus assigned to the vibrational relaxation process. The solvation process is insignificant for tetracene, even in protic solvents, as revealed from the invariant steady-state spectra among the solvents used. The slight dependence on solvent viscosity implies that the molecular rotation may couple weakly to the relaxation of vibrational energy. Contrary to *p*-terphenyl, the rate of vibrational relaxation for tetracene is not enhanced in protic solvents. However, a large isotopic effect in solvent MeOD and perdeuterated methanol (CD_3OD) was observed, showing a rather complex solute–solvent interaction for tetracene. The similar isotopic effect for MeOD and CD_3OD indicates that the vibrational modes associated with methyl group play a minor role in vibrational relaxation process. Note that the τ_2 obtained in MeOD and CD_3OD is nearly two times that in aprotic solvents, revealing a minor hydrogen bonding effect. Considering such a large excess energy ($>15\,000\text{ cm}^{-1}$), it is possible that the vibrational relaxation is not solely dominated by the low-frequency friction modes, but the high-frequency vibrational modes of OH are also responsible for mediating the vibrational energy into solvent environment.

The three molecules under investigation have similar molecular structure but varied in rigidity, from which we observed a largely different sensitivity of the rate of vibrational relaxation to

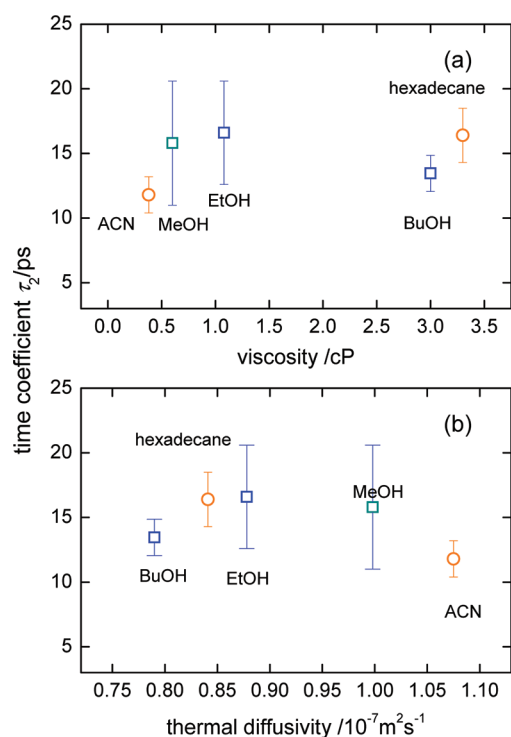


Figure 10. Relaxation time constant τ_2 of tetracene in aprotic (circle) and protic (square) solvents versus (a) viscosity and (b) thermal diffusivity.

the solvent environment as well as the solvent isotope effect. The comparison of experimental results with the structural modification provides some physical insight into the vibrational relaxation process despite lacking of the knowledge of detailed frequency-resolved dynamics of these molecules in their S_1 state. For *p*-terphenyl, the vibrational relaxation shows a linear dependence on solvent viscosity in aprotic solvents, indicating that the molecular rotation is coupled to vibration. A more viscous solvent hampers molecular rotation; the vibrational energy transfer is consequently slow. Tetracene displays a weak dependence on solvent viscosity. Values of τ_2 obtained for tetracene are slightly greater than those for *p*-terphenyl, although for tetracene the vibrational energy equivalent to $\sim 15\,000\text{ cm}^{-1}$ is much greater than that, $\sim 5600\text{ cm}^{-1}$, for *p*-terphenyl. We expect relaxation to be more rapid for a system with greater excess vibrational energy. For these two molecules of similar shape and size, we expect similar principal rotational structures of the whole molecule. The additional torsional motion of biphenyl in *p*-terphenyl has hence an effect of accelerating the vibrational relaxation in aprotic solvents; this motion plays a greater role in promoting vibrational cooling than the energy dissipation of the hot solvent. With no torsional motion of biphenyl, *dm*-terphenyl has a rate of vibrational cooling greater than that of *p*-terphenyl for approximately the same excess vibrational energy, perhaps because the methyl rotation with extra angular momentum results in efficient transfer of vibrational energy to the solvents. The rate of vibrational cooling of *dm*-terphenyl hence shows no clear dependence on either the viscosity of the solvent.

5. CONCLUSIONS

We measured femtosecond time-resolved fluorescence of *p*- and *dm*-terphenyl and tetracene dissolved in solvents of varied

physical properties — viscosity, dielectric constant, and protic/aprotic nature. By examining the solvent dependence of the dynamics observed, we fully characterized the photophysical processes of these three molecules. *p*-Terphenyl undergoes ultrafast intramolecular redistribution of vibrational energy, followed by a conformational relaxation in excited-state S_1 . The rate of conformational relaxation is accelerated in a protic solvent but is lower in methanol-OD than in methanol; this isotopic effect is explained to result from the variation in the large-wavenumber bath modes of the solvent environment, especially the librational frequencies of the OH moiety. Similarly, *dm*-terphenyl undergoes a rapid IVR, followed by vibrational cooling at 5.2–8.8 ps. Because the torsional conformational change in biphenyl is inhibited by the steric hindrance of the methyl substituents, this torsional motion is expected to have no effect on coupling to vibrational relaxation. Nevertheless, the faster rate of relaxation of *dm*-terphenyl than for *p*-terphenyl is observed.

On excitation at 266 nm, tetracene is initially excited to state S_3 ; the subsequent internal conversion $S_3 \rightarrow S_1$ is completed with a time constant near 0.1 ps. In the S_1 manifold, tetracene, which acquires a large amount of excess vibrational energy $\sim 15\,000\text{ cm}^{-1}$, undergoes vibrational relaxation with a time constant of 11.8–16.6 ps. A lack of clear dependence on solvent thermal diffusivity and viscosity implies that the vibrational relaxation is not limited solely by the individual motions in solvent. A large isotopic effect in the rate of vibrational relaxation for MeOH versus deuterated methanol indicates that vibrational modes with great energy such as O–H stretch might be more effective accepting modes in energy transfer. For the three molecules studied, in general, we observed an isotopic effect in the relaxation rate of vibrational energy—slower rate in deuterated methanol.

■ ASSOCIATED CONTENT

S Supporting Information. Femtosecond time-resolved fluorescence decay curves and the exponential fits for tetracene, *p*-terphenyl, and *dm*-terphenyl. This material is available free of charge via the Internet at <http://pubs.acs.org>.

■ AUTHOR INFORMATION

Corresponding Author

*E-mail: icchen@mx.nthu.edu.tw.

■ ACKNOWLEDGMENT

The National Science Council of Republic of China provided support for this research, and the National Center for High-Performance Computing, Taiwan, provided support for computing facilities.

■ REFERENCES

- (1) Rettig, W.; Maus, M. *Conformational Analysis of Molecules in Excited States*; Waluk, J., Ed.; Wiley-VCH: New York, 2000.
- (2) Elles, C. G.; Bingemann, D.; Heckscher, M. M.; Crim, F. F. *J. Chem. Phys.* **2003**, *118*, 5587.
- (3) Hare, P. M.; C.-Hernández, C. E.; Kohler, B. *J. Phys. Chem. B* **2006**, *110*, 18641.
- (4) Ohta, H.; Naitoh, Y.; Tominaga, K.; Yoshihara, K. *J. Phys. Chem. A* **2001**, *105*, 3973.
- (5) Charvet, A.; Aßmann, J.; Abel, B. *J. Phys. Chem. A* **2001**, *105*, 5071.
- (6) Schultz, S. L.; Qian, J.; Jean, J. M. *J. Phys. Chem. A* **1997**, *101*, 1000.
- (7) Seifert, G.; Graener, H. *J. Chem. Phys.* **2007**, *127*, 224505.

- (8) Sluch, M. I.; Godt, A.; Bunz, U. H. F.; Berg, M. A. *J. Am. Chem. Soc.* **2001**, *123*, 6447.
- (9) Cailleau, H.; Baudour, J. L.; Meinel, J.; Dworkin, A.; Moussa, F.; Zeyen, C. M. E. *Faraday Discuss.* **1980**, *69*, 7.
- (10) Weiss, E. A.; Tauber, M. J.; Kelley, R. F.; Ahrens, M. J.; Ratner, M. A.; Wasielewski, M. R. *J. Am. Chem. Soc.* **2005**, *127*, 11842.
- (11) Mallick, P. K.; Chattopadhyay, S.; Sett, P. *Chem. Phys. Lett.* **2000**, *331*, 215.
- (12) Takei, Y.; Yamaguchi, T.; Osamura, Y.; Fuke, K.; Kaya, K. *J. Phys. Chem.* **1988**, *92*, 577.
- (13) Mank, D.; Raytchev, M.; Amthor, S.; Lambert, C.; Fiebig, T. *Chem. Phys. Lett.* **2003**, *376*, 201.
- (14) Leonard, J. D.; Gustafson, T. L. *J. Phys. Chem. A* **2001**, *105*, 1724.
- (15) Tan, X.; Gustafson, T. L.; Lefumeux, C.; Burdzinski, G.; Buntinx, G.; Poizat, O. *J. Phys. Chem. A* **2002**, *106*, 3593.
- (16) Liu, K.-L.; Lee, S.-J.; Chen, I.-C.; Hsu, C.-P.; Yeh, M.-Y.; Luh, T.-Y. *J. Phys. Chem. A* **2009**, *113*, 1218.
- (17) Ladanyi, B. M.; Stratt, R. M. *J. Chem. Phys.* **1999**, *111*, 2008.
- (18) Chorny, I.; Benjamin, I. *J. Mol. Liq.* **2004**, *110*, 133.
- (19) Hino, S.; Seki, K.; Inokuchi, H. *Chem. Phys. Lett.* **1975**, *36*, 335.
- (20) Wakayama, N. I. *Chem. Phys. Lett.* **1980**, *70*, 397.
- (21) Akiyama, M. *Spectrochim. Acta* **1980**, *40A*, 367.
- (22) Swiatkowski, G.; Menzel, R.; Rapp, W. *J. Lumin.* **1987**, *37*, 183.
- (23) Sarkar, N.; Takeuchi, S.; Tahara, T. *J. Phys. Chem. A* **1999**, *103*, 4808.
- (24) Fujino, T.; Arzhantsev, S. Y.; Tahara, T. *J. Phys. Chem. A* **2001**, *105*, 8123.
- (25) Lim, E. C.; Li, Y. H. *J. Chem. Phys.* **1970**, *52*, 6416.
- (26) Westenhoff, S.; Beenken, W. J. D.; Friend, R. H.; Greenham, N. C.; Yartsev, A.; Sundström, V. *Phys. Rev. Lett.* **2006**, *97*, 166804.
- (27) Frisch, M. J.; Trucks, G. W.; Schlegel, H. B.; Scuseria, G. E.; Robb, M. A.; Cheeseman, J. R.; Montgomery, J. A., Jr.; Vreven, T.; Kudin, K. N.; Burant, J. C.; Millam, J. M.; Iyengar, S. S.; Tomasi, J.; Barone, V.; Mennucci, B.; Cossi, M.; Scalmani, G.; Rega, N.; Petersson, G. A.; Nakatsuji, H.; Hada, M.; Ehara, M.; Toyota, K.; Fukuda, R.; Hasegawa, J.; Ishida, M.; Nakajima, T.; Honda, Y.; Kitao, O.; Nakai, H.; Klene, M.; Li, X.; Knox, J. E.; Hratchian, H. P.; Cross, J. B.; Bakken, V.; Adamo, C.; Jaramillo, J.; Gomperts, R.; Stratmann, R. E.; Yazyev, O.; Austin, A. J.; Cammi, R.; Pomelli, C.; Ochterski, J. W.; Ayala, P. Y.; Morokuma, K.; Voth, G. A.; Salvador, P.; Dannenberg, J. J.; Zakrzewski, V. G.; Dapprich, S.; Daniels, A. D.; Strain, M. C.; Farkas, O.; Malick, D. K.; Rabuck, A. D.; Raghavachari, K.; Foresman, J. B.; Ortiz, J. V.; Cui, Q.; Baboul, A. G.; Clifford, S.; Cioslowski, J.; Stefanov, B. B.; Liu, G.; Liashenko, A.; Piskorz, P.; Komaromi, I.; Martin, R. L.; Fox, D. J.; Keith, T.; Al-Laham, M. A.; Peng, C. Y.; Nanayakkara, A.; Challacombe, M.; Gill, P. M. W.; Johnson, B.; Chen, W.; Wong, M. W.; Gonzalez, C.; Pople, J. A. *Gaussian 03*, revision D.01; Gaussian, Inc.: Wallingford, CT, 2004.
- (28) De Belder, G.; Jordens, S.; Lor, M.; Schweitzer, G.; De, R.; Weil, T.; Herrmann, A.; Wiesler, U. K.; Müllen, K.; De Schryver, F. C. *J. Photochem. Photobiol. A* **2001**, *145*, 61.
- (29) Baskin, J. S.; Banares, L.; Pedersen, S.; Zewail, A. H. *J. Phys. Chem.* **1996**, *100*, 11920.
- (30) Hornig, J. S.; Gardecki, J. A.; Papazyan, A.; Maroncelli, M. *J. Phys. Chem.* **1995**, *99*, 17311.
- (31) Fleming, G. R.; Cho, M. *Annu. Rev. Phys. Chem.* **1996**, *47*, 109.
- (32) Jimenez, R.; Fleming, G. R.; Kumar, P. V.; Maroncelli, M. *Nature* **1994**, *369*, 471.
- (33) Reynolds, L.; Gardecki, J. A.; Frankland, S. J. V.; Horng, M. L.; Maroncelli, M. *J. Phys. Chem.* **1996**, *100*, 10337.
- (34) Oskoue, A. A.; Bräm, O.; Cannizzo, A.; van Mourik, F.; Tortschanoff, A.; Chergui, M. *Chem. Phys.* **2008**, *350*, 104.
- (35) Assmann, J.; von Benten, R.; Charvat, A.; Abel, B. *J. Phys. Chem. A* **2003**, *107*, 1904.
- (36) Nesbitt, D. J.; Field, R. W. *J. Phys. Chem.* **1996**, *100*, 12735.
- (37) Iwata, K.; Hamaguchi, H. *J. Phys. Chem. A* **1997**, *101*, 632.
- (38) Pigliucci, A.; Duvanel, G.; Daku, L. M. L.; Vauthey, E. *J. Phys. Chem. A* **2007**, *111*, 6135.
- (39) Rostkier-Edelstein, D.; Graf, P.; Nitzan, A. *J. Chem. Phys.* **1997**, *107*, 10470.
- (40) Owrutsky, J. C.; Raftery, D.; Hochstrasser, R. M. *Annu. Rev. Phys. Chem.* **1994**, *45*, 519.
- (41) Sando, G. M.; Zhong, Q.; Owrutsky, J. C. *J. Chem. Phys.* **2004**, *121*, 2158.
- (42) Deng, Y.; Stratt, R. M. *J. Chem. Phys.* **2002**, *117*, 1735.
- (43) Morita, A.; Kato, S. *J. Chem. Phys.* **1998**, *109*, 5511.
- (44) Terazima, M. *Chem. Phys. Lett.* **1999**, *305*, 189.
- (45) Schwarzer, D.; Troe, J.; Votsmeier, M.; Zerezke, M. *J. Chem. Phys.* **1996**, *105*, 3121.
- (46) Yamaguchi, T.; Kimura, Y.; Hirota, N. *J. Chem. Phys.* **2000**, *113*, 2772.
- (47) Kimura, Y.; Yamamoto, Y.; Terazima, M. *J. Chem. Phys.* **2005**, *123*, 054513.
- (48) Middleton, C. T.; Cohen, B.; Kohler, B. *J. Phys. Chem. A* **2007**, *111*, 10460.
- (49) Falk, M.; Whalley, E. *J. Chem. Phys.* **1961**, *34*, 1554.
- (50) Skaf, M. S.; Fonseca, T.; Ladanyi, B. M. *J. Chem. Phys.* **1993**, *98*, 8929.
- (51) Venables, D. S.; Chiu, A.; Schmuttenmaer, C. A. *J. Chem. Phys.* **2000**, *113*, 3243.
- (52) Rey, R.; Moller, K. B.; Hynes, J. T. *Chem. Rev.* **2004**, *104*, 1915.
- (53) Iwata, A.; Hamaguchi, H. *J. Raman Spectrosc.* **1994**, *25*, 615.
- (54) Englman, R.; Jortner, J. *J. Mol. Phys.* **1970**, *18*, 145.